Dalton Transactions

ROYAL SOCIETY OF CHEMISTRY

PAPER

View Article Online
View Journal | View Issue

Check for updates

Cite this: *Dalton Trans.*, 2025, **54**, 1495

Pd-catalysed C–H bond functionalisation route to 1,2-dihydroferroceno[*c*]isoquinoline and its annellated derivatives and the reactivity of these compounds†

Věra Varmužová,[a] Ivana Císařová,[a] Jiří Schulz,[a] Květa Kalíková[b] and Petr Štěpnička *[a]

Received 1st November 2024,
Accepted 28th November 2024

DOI: 10.1039/d4dt03063j

rsc.li/dalton

C–H bond functionalisation has developed into a powerful synthetic methodology that is applicable to a wide array of substrates, including organometallic compounds. In this study, racemic, planar-chiral 1,2-dihydroferroceno[*c*]isoquinoline and analogous helical compounds with one or two additional *ortho*-fused benzene rings were synthesised by palladium-catalysed C–H bond activation/cyclisation of *N*-[(bromoaryl)methyl]-*N*-(methylsulfonyl)aminoferrocenes. These starting materials are readily accessible from $FcNHSO_2Me$ (Fc = ferrocenyl) and appropriate vicinal bromo-(bromomethyl)arenes. The racemic products were successfully enantioseparated using chiral chromatography and the representative compound, 1,2-dihydro-2-(methylsulfonyl)ferroceno[*c*]isoquinoline, was converted to the unstable ferroceno[*c*]isoquinoline and further used to prepare a heterobimetallic, Fe/Ru bis-metallocene complex *via* a reaction with $[(\eta^5\text{-}C_5Me_5)Ru(MeCN)_3][PF_6]$. All compounds were characterised by spectroscopic methods (NMR, FTIR, and UV-vis) and mass spectrometry and, in most cases, the structures were determined by single-crystal X-ray diffraction analysis. In addition, the representative compounds were examined by cyclic voltammetry, and the results were rationalised with the aid of DFT calculations.

Introduction

Transition metal-catalysed C–H bond functionalisation enables the synthesis of more complex molecules from accessible C–H substrates through the formation of new C–C and C–heteroatom bonds. Compared with conventional methods, this approach is more atom-economic but also more challenging due to the generally low reactivity of the C–H bonds. Hence, harsh reaction conditions or carefully designed catalysts and various directing groups are typically needed to achieve satisfactory results.[1]

In ferrocene chemistry,[2] reactions involving directed C–H functionalisation provide alternative access to planar chiral compounds.[3] In this respect, *ortho*-condensed systems in which the ferrocene cyclopentadienyl rings are annellated with a (hetero)aromatic moiety are particularly interesting. Although the first compounds of this type, bis(η^5-indenyl)iron(II) (**A**),[4] ferroceno[2,3]indenone (**B**)[5] and the corresponding indene **C**[6] (Scheme 1, top), were prepared shortly after the discovery of ferrocene itself,[2a] interest in these compounds was renewed with the advent of synthetic methods based on the C–H bond activation. Thus, compound **B** was obtained using Pd-catalysed cyclisation of (2-halobenzoyl)ferrocenes,[7] and a similar method was utilised to synthesise similar compounds with a terminal pyridine ring.[8,9] More recently, routes based on asymmetric, Pd-mediated C–H bond functionalisation led to ferrocenopyridines (**D**),[10] quinoline derivatives (**E** and **F**),[11] and (iso)quinolinones (**G**)[12] (Scheme 1).

In our research, we were inspired by the recently disclosed[13] one-pot cascade reaction involving nucleophilic alkylation, C–H bond activation, and aromatisation that converted *N*-sulfonyl aryl amines into phenanthridines (Scheme 1, bottom), and decided to apply this approach to the synthesis of analogous ferrocene-based compounds. The results from our study are reported here.

[a]*Department of Inorganic Chemistry, Faculty of Science, Charles University, Hlavova 2030, 128 00 Prague, Czech Republic. E-mail: stepnic@natur.cuni.cz*
[b]*Department of Physical and Macromolecular Chemistry, Faculty of Science, Charles University, Hlavova 2030, 128 00 Prague, Czech Republic*

†Electronic supplementary information (ESI) available: Complete experimental details, including all synthetic procedures and characterisation data, details on electrochemical measurements, structure determination and DFT calculations, Cartesian coordinates of DFT-optimised structures and copies of the NMR spectra. CCDC 2389173–2389180. For ESI and crystallographic data in CIF or other electronic format see DOI: https://doi.org/10.1039/d4dt03063j

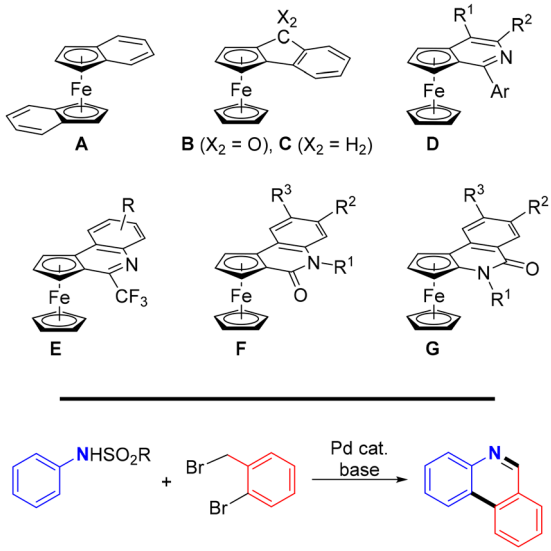

Scheme 1 (top) Examples of annellated ferrocenes relevant to this study and (bottom) Pd-catalysed cascade reaction producing phenanthridines from *N*-sulfonyl anilines.

Results and discussion

Synthesis of 1,2-dihydro-2-(methylsulfonyl)ferroceno[*c*] isoquinoline and analogues with an extended π-system

The starting material, *viz.* [(methylsufonyl)amino]ferrocene (**1**), was prepared by the reaction of aminoferrocene ($FcNH_2$, Fc = ferrocenyl) with methanesulfonyl chloride in tetrahydrofuran (THF) in the presence of pyridine.[14] It was isolated as an air-stable, orange crystalline solid in 83% yield after column chromatography. Unfortunately, the direct reaction of **1** with 2-bromobenzyl bromide (**2a**) (Scheme 2) did not proceed under the conditions reported for the aforementioned direct synthesis of phenanthridines[13] despite numerous attempts.[15]

To achieve our synthetic goal, we then resorted to a stepwise approach and employed a "preassembled" intermediate. In the first step, compound **1** was alkylated with **2a** in the presence of Cs_2CO_3 in acetonitrile at 70 °C to produce *N*-(2-bromobenzyl)sulfonamide **3a** in a 94% isolated yield (Scheme 3; *N.B.* a similar reaction in *N*,*N*-dimethylformamide gave **3a** in only 45% yield). Compound **3a** already reacted under the conditions provided in Scheme 2 to produce a mixture of the targeted compound **4a** and the corresponding dehalogenation product **5a** (see Scheme 3). However, as the majority of the starting material **3a** (71%) remained unconsumed, we pursued a more efficient catalyst. Indeed, upon replacing $Pd(tfa)_2$ with Generation 3 Buchwald's Pd precatalyst **BG3**[16] (Scheme 4), increasing the catalyst amount to 10 mol% Pd and extending the reaction time, **3a** was fully converted into a 94 : 6 mixture of **4a** and **5a** (Table 1). With the following optimisation experiments, we tried to increase the reaction efficiency (*i.e.*, the conversion and selectivity towards the cyclisation product **4a**) at a *lower* catalyst amount (1 mol% Pd).

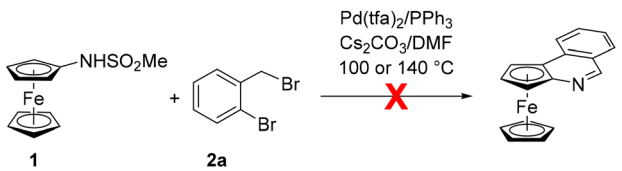

Scheme 2 Attempted direct annulation of **1** with **2a**. Conditions: **1** (0.36 mmol), **2a** (0.36 mol), $Pd(tfa)_2$ (5 mol%), PPh_3 (20 mol%), and Cs_2CO_3 (4 equiv. *vs.* **1**) were reacted in anhydrous *N*,*N*-dimethylformamide (4 mL) at 100 or 140 °C for 1–2 days; $Pd(tfa)_2$ = palladium(II) trifluoromethanesulfonate.

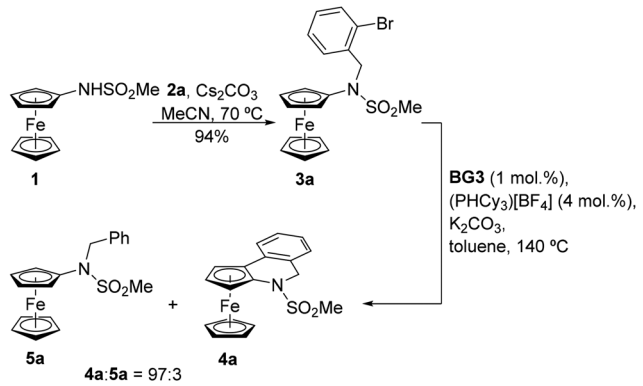

Scheme 3 Synthesis and Pd-catalysed cyclisation of **3a**.

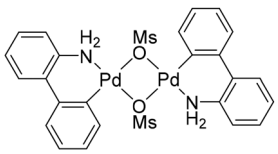

Scheme 4 Precatalyst **BG3**.

Table 1 Optimisation of the reaction conditions for the conversion of **3a** to **4a**[a]

Pd source [mol%]	Ligand [equiv.][b]	Base	Solvent	Time [h]	**3a** : **4a** : **5a**
$Pd(tfa)_2$ [5]	PPh_3 [4]	Cs_2CO_3	DMF	13	71 : 21 : 8
BG3 [10]	PPh_3 [4]	AcOK	Toluene	144	0 : 94 : 6
$Pd(OAc)_2$ [1]	PPh_3 [2]	AcOK	Toluene	24	68 : 30 : 2
$Pd(OAc)_2$ [1]	PPh_3 [4]	AcOK	Toluene	24	60 : 38 : 2
BG3 [1]	PPh_3 [2]	AcOK	Toluene	24	15 : 83 : 2
BG3 [1]	PPh_3 [4]	AcOK	Toluene	24	2 : 94 : 4
BG3 [1]	PPh_3 [4]	AcONa	Toluene	24	76 : 20 : 4
BG3 [1]	PPh_3 [4]	AcOCs	Toluene	24	42 : 55 : 3
BG3 [1]	PPh_3 [4]	AcOK	DCE	24	79 : 20 : 1
BG3 [1]	PPh_3 [4]	K_2CO_3	Toluene	24	66 : 29 : 5
BG3 [1]	PPh_3 [4]	K_3PO_4	Toluene	24	58 : 38 : 4
BG3 [1]	$PCy_3{\cdot}H[BF_4]$ [4]	AcOK	Toluene	24	0 : 97 : 3
BG3 [1]	$PCy_3{\cdot}H[BF_4]$ [4]	K_2CO_3	Toluene	24	0 : 97 : 3

[a] All reactions were performed at 140 °C. DMF = *N*,*N*-dimethylformamide, DCE = 1,2-dichloroethane, Cy = cyclohexyl; the structure of **BG3** is shown in Scheme 4. [b] Equivalents of the phosphine ligand per palladium.

The results shown in Table 1 confirm the generally better efficiency of the catalysts generated from **BG3** compared to those resulting from palladium carboxylates. A further improvement was noted upon changing triphenylphosphine to the more basic tricyclohexylphosphine (PCy_3; the phosphine was generated *in situ* from the easier-to-handle, air-stable phosphonium salt and the base, which was used in excess),[17] whereas the amount of auxiliary phosphine (2 *vs.* 4 equiv. per Pd) had a lower impact on the reaction course. Potassium acetate or carbonate were identified as suitable bases, and the reactions performed in toluene proceeded better than those in *N*,*N*-dimethylformamide and 1,2-dichloroethane. Eventually, the combination of a **BG3**/PCy_3 catalyst (1 mol% Pd, Pd : P = 1 : 4) and K_2CO_3 in toluene enabled the cyclisation with full conversion of the starting material and 97% selectivity for **4a** when the reaction was performed in a pressure tube at 140 °C. Compounds **4a** and **5a** could not be efficiently separated by column chromatography; a pure sample of **4a** was obtained by crystallisation from THF/hexane.

Having established a reliable route to **4a**, we focused on the synthesis of congeners with a larger conjugated π-system. Extension of the aromatic system by one fused benzene ring was easily achieved. The required starting material **3b** was obtained in good yield (>90%) by alkylation of **1** with 1-bromo-2-(bromomethyl)naphthalene (**2b**) under conditions used to prepare **3a** (Scheme 5). Amide **3b** was subsequently cyclised under the developed conditions ($BG3/PCy_3{\cdot}H[BF_4]$, K_2CO_3, toluene, 140 °C/24 h) to produce the corresponding annellated compound **4b** contaminated with a minor amount of the dehalogenation product **5b** (11%; Scheme 5). Even in this case, the side product could not be efficiently separated by column chromatography; however, the crystallisation of the product mixture from hot heptane produced two types of crystals, which were manually separated.

The alkylating agent needed for the synthesis of the compound possessing three fused benzene rings, 4-bromo-3-(bromomethyl)phenanthrene (**2c**), was synthesised from the commercially available 2,3-dihydrophenanthren-4(1*H*)-one (**8**). This compound was converted to 4-bromophenanthrene-3-carbaldehyde (**10**) in two steps using a literature procedure.[18] Next, the aldehyde was reduced to the corresponding alcohol **11** using $Na[BH_4]$ in THF/methanol, and the alcohol was brominated with PBr_3 to produce the targeted dibromide **2c** (Scheme 6). The yield over the last two synthetic steps was 56%.

Alkylation of **1** with **2c** smoothly proceeded to produce starting material **3c**. However, the following cyclisation step required additional optimisation to proceed satisfactorily. In particular, the reaction had to be performed in anhydrous 1,4-dioxane, in which it proceeded with full conversion and afforded an 80 : 20 mixture of **4c** and **5c** (Scheme 5; *N.B.* the amount of the dehalogenated side product **5c** was considerably greater when non-strictly dried and deoxygenated solvent was employed).

With compounds **4a–c** in hand, we attempted to remove the sulfonate group and to synthesise the corresponding, fully aromatic compounds, ferrocenoisoquinolines. Following a literature procedure for NH group deprotection,[19,20] a mixture of **4a** and **5a** (97 : 3) was treated with sodium bis(2-methoxyethoxy) aluminium hydride (Red-Al) in toluene. However, instead of the expected sulfonate group removal, this reaction directly produced ferrocenoisoquinoline **6a** in a 30–35% yield (Scheme 7).

Next, we tried to "deprotect" the **4a**/**5a** mixture using a base. No reaction was observed when the mixture was refluxed with 5% KOH in methanol or heated with Cs_2CO_3 in *N*,*N*-dimethylformamide at 140 °C. Eventually, the deprotection, again with concomitant aromatisation, was achieved upon treating the **4a**/**5a** mixture with potassium *tert*-butoxide (5 equiv.) in toluene at 100 °C for 2 h. The conversion of **4a** into **6a** was indicated by a pronounced colour change from orange to deep red. Compound **6a** was isolated by chromatography as a red solid with a 71% yield over the two steps (*i.e.*, from **3a**). A small amount of impure Schiff base **7a** was also obtained and adequately identified.

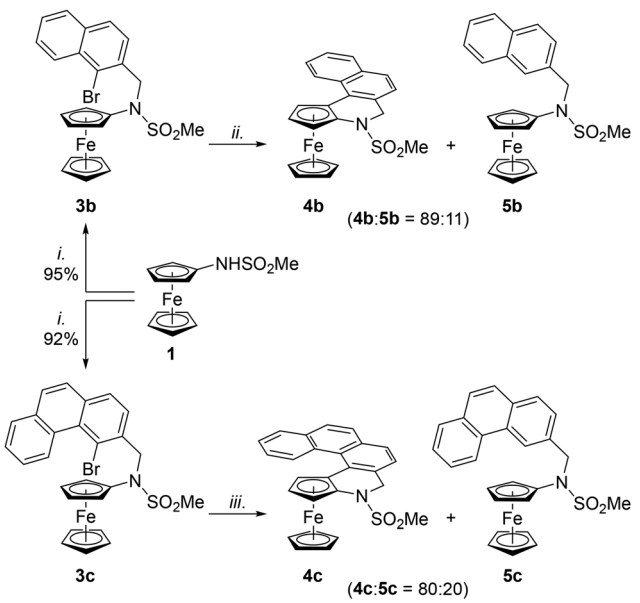

Scheme 5 Synthesis and cyclisation of **3b** and **3c**. Conditions: i. **2b** or **2c**, Cs_2CO_3, MeCN, 70 °C/3 h; ii. **BG3** (1 mol%), $(PHCy_3)[BF_4]$ (Pd : P = 1 : 4), toluene, 140 °C/24 h; iii. same as ii. except that 1,4-dioxane was used as the solvent.

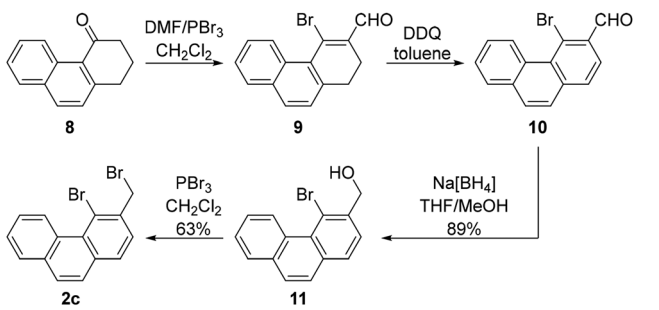

Scheme 6 Synthesis of 4-bromo-3-(bromomethyl)phenanthrene (**2c**).

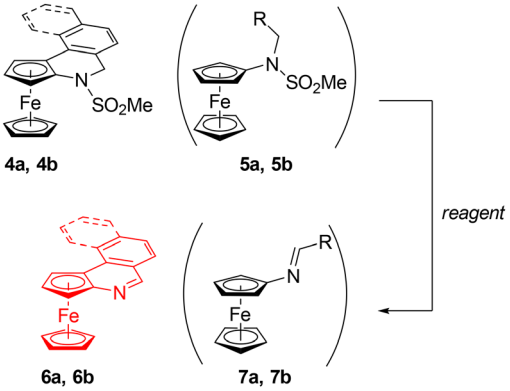

Scheme 7 Synthesis of ferrocenoisoquinolines **6** (R = Ph (**a**), 2-naphthyl (**b**); see text for details).

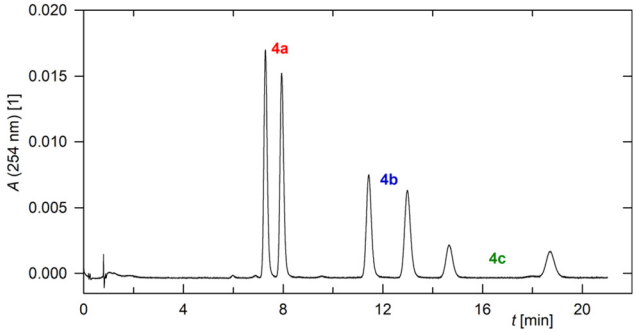

Fig. 1 SFC chromatogram of an equimolar **4a–4c** mixture (Lux® i-Amylose-3 column, 150 × 4.6 mm, particle size 3 μm, CO_2–methanol 80 : 20, 2 mL min^{-1}, 40 °C, back pressure regulator 2000 psi, UV detection at 254 nm).

Unfortunately, compound **6a** was unstable and readily converted into an insoluble black solid. The decomposition was faster in a solution (especially in halogenated solvents), which precluded the crystallisation of this compound. Solid samples could be stored at −18 °C but still had to be freshly purified by chromatography before use. Efforts to prepare a more stable derivative by the methylation of **6a** with MeI or $[Me_3O][BF_4]$ and by the reaction with picric acid were unsuccessful; these reactions uniformly led to dark intractable solids.

The mixture of **4b** and **5b** also reacted with *t*-BuOK to give a mixture of the respective aromatised compounds **6a** and **7b** (Scheme 7). These compounds were separated by column chromatography; the yield of **6b** was 67%. However, compound **6b** was even less stable than **6a** and, hence, no further experiments focused on the properties and reactivity of these aromatic derivatives were made.

Notably, our attempts to conduct the cyclisation reaction asymmetrically were unsuccessful. The cyclisation reactions were performed similarly to the synthesis of the racemic compounds but with catalysts based on **BG3** and common chiral phosphine ligands (see ESI, Scheme S1†) that were successfully applied in asymmetric, Pd-catalysed reactions leading to chiral helicenes.[21] In the present case, however, these conditions either entirely failed (for (*S*)-BINAP and (*R*)-H_8BINAP; yields <5%) or led to racemic cyclisation product **4a** (for (*S*)-SEGPHOS and (*R*)-2,2′-bis[bis(3,5-dimethylphenyl)phosphino]-6,6′-dimethoxybiphenyl).

Therefore, the separation of the enantiomers was examined using supercritical fluid chromatography (SFC)[22] on a modified amylose column with a CO_2–methanol mixture as the eluent (for details, see the ESI†). Under these conditions, the enantiomers of **4a–4c** were baseline resolved, with increasing amounts of CO_2 in the mobile phase (70 : 30 → 90 : 10) improving peak resolution. The retention time increased with increasing molecular weight, as expected. Thus, all six species present in a model mixture of the three compounds **4a–4c** could be separated (Fig. 1). Efficient separation of the enantiomers of **4a** was also achieved by conventional HPLC analysis on the same column using *n*-heptane/2-propanol (80/20) as the eluent.

Structural characterisation of the prepared compounds

All compounds were characterised using a combination of electrospray ionisation mass spectrometry, elemental analysis (conventional or from high-resolution MS), and UV-vis, FTIR and NMR spectroscopies. In addition, the solid-state structures of compounds **1**, **3a–c**, and **4a–c** were determined by single-crystal X-ray diffraction analysis. Only the structures of the annellated compounds **4a–c** are presented here; other structures are discussed in the ESI.†

The identities of the prepared compounds were initially verified by the mass spectra, which revealed ions due to the molecular ions (M^+) or their simple adducts ($[M + H]^+$ or $[M + Na]^+$), whereas the individual structures were corroborated by the NMR spectra. In particular, the ^{1}H NMR spectra displayed characteristic sets of signals due to the ferrocene moiety. Besides a strong singlet of the C_5H_5 ring, two virtual triplets arising from the AA′BB′ spin system were observed for **1**, **3a–c** and **5a–c**, whereas an AMX pattern due to the C_5H_3 ring was detected in the spectra of the annellated compounds **4a–c**, **6a** and **6b**. The methylene protons in **3a–c** gave rise to singlets at δ_H 4.9–5.2, while the planar chiral compounds **4a–c**, where these protons become diastereotopic, displayed AB doublets at δ_H 4.9–5.3 (only compound **4b** showed a broad singlet). The corresponding ^{13}C NMR methylene signals were detected at δ_C 56–58 and δ_C 51–53, respectively. The ^{13}C NMR spectra revealed all other expected signals, including the low-field resonance due to ferrocene C^{ipso}–N (**3a–c**: $\delta_C \approx 101$; **4a–c**: $\delta_C \approx 97$; *cf.* δ_C 105.6 for aminoferrocene in $CDCl_3$ [23]).

The NMR spectra also showed signals at approximately δ_H 2.4–3.0 and $\delta_C \approx 37$, assigned to the sulfonamide moiety. Its presence was further confirmed by intense absorption bands at approximately 1340 ($\nu_{as}SO_2$) and 1160 (ν_sSO_2) cm^{-1} in the FTIR spectra.[24] For the parent compound **1**, the sulfonate bands were shifted to lower energies (maxima at 1307 and 1148 cm^{-1}), and the spectrum displayed a strong ν_{NH} band at 3245 cm^{-1}.[24]

The NMR spectra of isoquinolines **6a** and **6b** revealed diagnostic imine resonances at $\delta_H \approx 8.9–9.1/\delta_C \approx 157$ and the expected signals from the aromatic fragments. Furthermore, the colour change associated with the conversion of **4a** to **6a**,

reflecting the different extents of conjugation in these molecules, was nicely manifested in the UV-vis spectra (Fig. 2). The spectrum of **4a** displayed a band at 452 nm, which was ascribed to the forbidden d–d transition at the ferrocene unit[25] (*N.B.* ferrocene itself displays this band at 440 nm in an EtOH solution as well as in the gas phase).[26] A shoulder at a strong band extending from the UV region was also detected. For isoquinoline **6a**, the low-energy band was bathochromically shifted to 505 nm (albeit with a practically unchanged intensity), whereas the shoulder developed into a separate band at 398 nm.

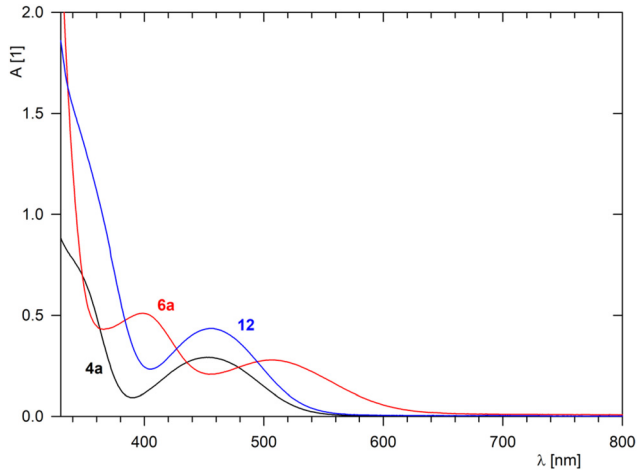

Fig. 2 UV-vis spectra of **4a**, **6a**, and complex **12** (c = 0.75 mM in dichloromethane, optical path 1 cm).

The structures of **4a**·0.25THF, **4b**, and **4c** determined by X-ray diffraction analysis are shown in Fig. 3, and the selected geometric parameters are listed in Table 2. The compounds were prepared and isolated as racemic mixtures and, correspondingly, crystallised with the symmetry of centric space groups ($P2_1/n$ or $P\bar{1}$). The asymmetric units of **4a**·0.25THF and **4b** contained two practically identical molecules (see the ESI†).

The combination of three types of rings (cyclopentadienyl, 1,2-dihydropyridine and benzene) made the structures of **4a–c** rather irregular compared with archetypal helicenes built exclusively from *ortho*-fused benzene rings.[27] In particular, the C5 atom and, to a lesser extent, the adjacent carbon C5a of the dihydropyridine moiety were displaced from the pivotal cyclopentadienyl plane (see the torsion angles in the ESI,

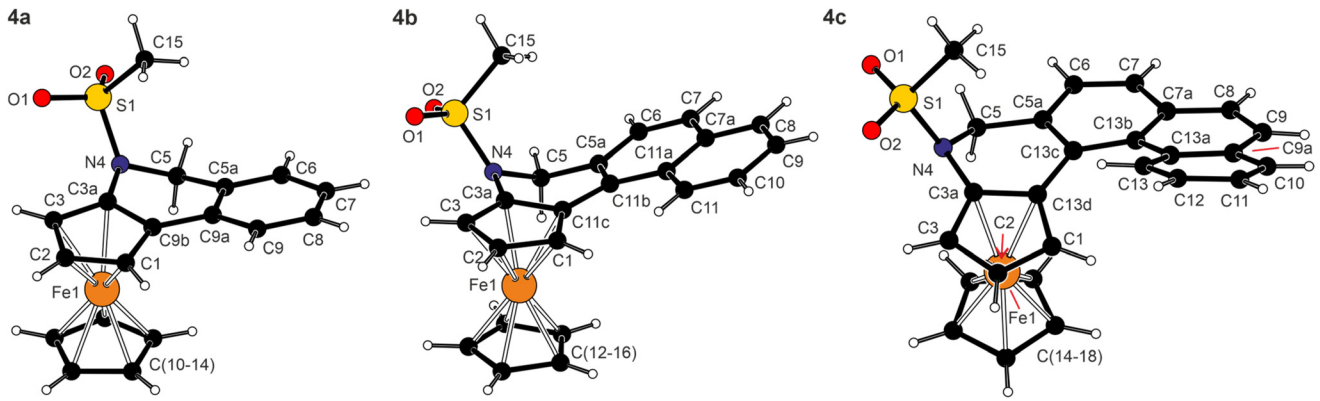

Fig. 3 Molecular structures of **4a** (molecule 1), **4b** (molecule 1) and **4c** (for displacement ellipsoid plots and additional structure diagrams, see the ESI†).

Table 2 Selected geometric parameters for **4a–c** (in Å and °)

Parameter[a]	**4a** (molecule 1)	**4a** (molecule 2)	**4b** (molecule 1)	**4b** (molecule 2)	**4c**
Fe–C (range)	2.027(2)–2.052(2)	2.041(1)–2.056(1)	2.022(8)–2.050(8)	2.01(1)–2.104(8)	2.026(1)–2.068(1)
Tilt	4.4(1)	0.44(9)	1.5(5)	6.2(6)	2.46(8)
N4–S1	1.646(1)	1.648(1)	1.638(6)	1.603(8)	1.646(1)
S1–O1/O2	1.433(1)/1.434(1)	1.434(1)/1.436(1)	1.430(6)/1.441(6)	1.421(6)/1.449(7)	1.434(1)/1.427(1)
O1–S1–O2	118.97(8)	119.21(7)	119.8(3)	118.8(4)	119.25(6)
N4–S1–C(Me)	107.34(8)	107.16(8)	106.7(4)	107.5(4)	106.87(7)
ϕ	12.79(9)	13.49(8)	20.7(4)	25.4(5)	42.44(7)
τ_1	−13.7(3)	−10.2(3)	17(1)	−22(2)	19.0(2)
τ_2	n.a.	n.a.	−9(1)	−8(1)	21.9(2)
τ_3	n.a.	n.a.	n.a.	n.a.	18.6(2)

[a] Definitions: ϕ is the dihedral angle between the substituted cyclopentadienyl ring and the plane of the *terminal* C_6H_4 ring; τ_1 is the torsion angle C1–C9b–C9a–C9 for **4a**, C1–C11c–C11b–C11a for **4b**, and C1–C13d–C13c–C13b for **4c**; τ_2 is the torsion angle C11c–C11b–C11a–C11 for **4b**, and C13d–C13c–C13b–C13a for **4c**; τ_3 is the torsion angle C13c–C13b–C13a–C13 in **4c**; tilt is the dihedral angle of the cyclopentadienyl least squares; and n.a. = not applicable.

Fig. S10†). This also resulted in tilting of the adjacent benzene ring [(C5a, C6–9, C9a) for **4a** and analogously in other compounds] by approximately 13° in **4a** and by 21–22° in **4b** and **4c**. However, this twisting alleviated steric collisions within the condensed ring system, thereby reducing the tendency towards a helical arrangement in smaller molecules of **4a** and **4b**. Most likely, the limit was exceeded upon the addition of yet another *ortho*-fused benzene ring, such as in **4c**; here, the rings were already arranged in a screw-like manner (see τ angles in Table 2). For example, the benzene rings in the phenanthrene fragment of **4c** were mutually tilted by 11.12(6)° (C5a–C13c *vs.* C7a–C13b) and 10.91(6)° (C7a–C13b *vs.* C9a–C13a), and the terminal C_6H_4 ring was twisted by 42.44(7)° from the C_5H_3 plane. In contrast, the carbon atoms in the entire naphthalene fragment of **4b** were coplanar within less than 0.1 Å. For all molecules, the sulfonate arm was directed above the ferrocene unit, and its oxygen atoms were oriented away from the ring system. The geometry of the N-SO_2Me fragment in **4a–c** remained similar to that in precursors **1** and **3a–c** (see the ESI†).

Synthesis of the Fe/Ru complex 12 and electrochemistry

Compound **4a** was further used to prepare heterobimetallic Fe/Ru complex **12** *via* a reaction with $[(\eta^5\text{-}C_5Me_5)Ru(MeCN)_3][PF_6]$[28] in 1,2-dichloroethane at 40 °C (Scheme 8). Evaporation followed by chromatography over an alumina column produced compound **12** as an orange solid in a 75% yield. A similar reaction with **6a** (in 1,2-dichloroethane or THF) led to a complete decomposition of the ferrocene derivative.

Complex **12** was spectroscopically characterised, and the solid-state structure of solvate **12**·$2CH_2Cl_2$ was established by X-ray diffraction analysis. The formation of **12** was indicated by the NMR spectra showing signals due to the introduced (η^5-C_5Me_5)Ru moiety (δ_H 1.83, δ_C 10.30 and 97.55 in acetone-d_6) and resonances expected for π-coordinated **4a**, especially the high-field signals due to the C_6H_4 ring (δ_H 6.06–6.31; δ_C 82.88–88.08 for the four CH groups, and 97.05/97.96 for C^{ipso}). The presence of the counterion was corroborated by a characteristic septet in the $^{31}P\{^1H\}$ NMR spectrum (δ_P −138.2, $^1J_{PF}$ = 708 Hz) and a broad intense $\nu_3(PF_6^-)$ band centred at approximately 845 cm^{-1} in the FTIR spectrum.[29] Notably, the coordination of (η^5-C_5Me_5)Ru^+ to **4a** did not change the UV-vis spectrum except for an increase in the intensity of the band at approximately 455 nm (see Fig. 2).

The structure of **12** (Fig. 4) consisted of two isoelectronic (cyclopentadienyl)metal fragments coordinated in an *anti*-fashion with respect to the bridging, non-conjugated bis-six electron donor ligand **4a**. The two metallocene moieties adopted their usual geometry (*cf.* the structure of $[(\eta^5\text{-}C_5Me_5)Ru(\eta^6\text{-}C_6H_6)][BPh_4]$[30]). While the π-bound rings in the ferrocene unit were tilted by 4.95(8)°, a smaller deformation was found for the (η^5-C_5Me_5)Ru(η^6-C_6H_4) fragment (0.86(7)°). The planes of the C_5H_3 and C_6H_4 rings were mutually tilted by 12.36(7)°; this value was similar to that in uncoordinated **4a** (in fact, the "molecule" of **4a** retained many of its structural features, including an overall conformation, upon coordination). Consistent with the Chatt–Dewar–Duncanson bonding model,[31] the C–C bonds in the C_6H_4 ring were elongated from 1.388(3)–1.405(2) Å in **4a** to 1.414(2)–1.427(2) Å in **12**.

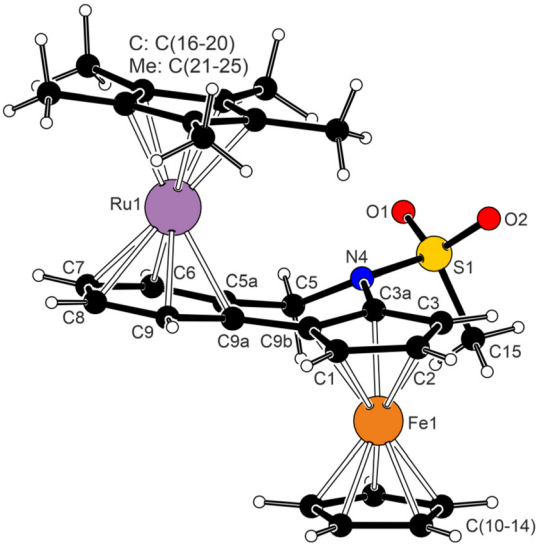

Fig. 4 View of the complex cation in the structure of **12**·$2CH_2Cl_2$. Selected distances and angles (in Å and °): Ru1–C5A 2.220(1), Ru1–C6 2.219(1), Ru1–C7 2.222(1), Ru1–C8 2.224(1), Ru1–C9 2.223(1), Ru1–C9A 2.237(1), Ru1–C(16–20) 2.182(1)–2.194(1), Fe–C 2.038(1)–2.063(2), S1–N4 1.646(1), S1–O1/2 1.430(1)/1.431(1), N4–S1–C15 106.37(7), O1–S1–O2 119.23(7).

In addition to spectroscopic and structural characterisation, representative compounds **1**, **3a**, **4a**, **6a**, and **12** were studied by cyclic voltammetry at a glassy carbon disc electrode in dichloromethane containing 0.1 M $Bu_4N[PF_6]$ as the supporting electrolyte. In the accessible potential range, the compounds underwent several redox transitions. Typically, the "primary" oxidations (Fig. 5) were followed by additional, ill-defined oxidation step(s) that were affected by adsorption phenomena and resulted in blocking of the electrode surface. Therefore, further attention was given only to the primary oxidations.

For **1** and **3a**, this oxidation was observed as a standard, one-electron reversible transition at $E^{o\prime}$ = 0.00 and 0.06 V *vs.* the ferrocene–ferrocenium reference,[32] respectively (see the ESI†). These values, close to zero, indicated that the electronic properties of the ferrocene core were only marginally perturbed by the appended substituents; the former value also corresponded with the Hammett σ_p constant for the $HNSO_2Me$ group, close to zero (0.03).[33]

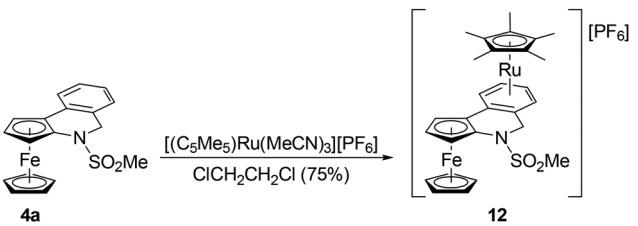

Scheme 8 Synthesis of complex **12**.

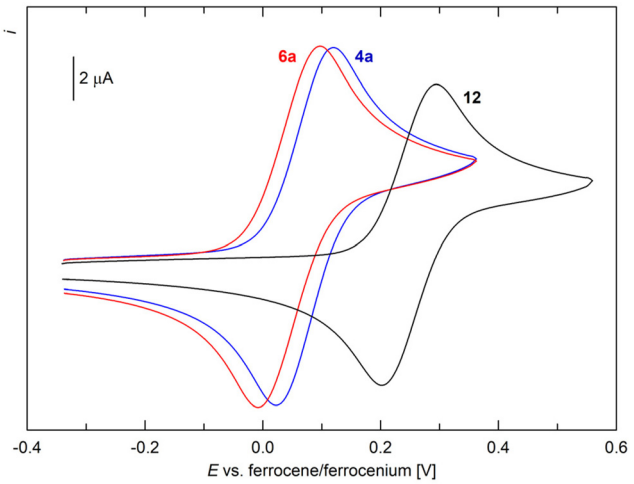

Fig. 5 Cyclic voltammograms of **4a**, **6a**, and **10** as recorded on a glassy carbon disc electrode in CH_2Cl_2 (0.1 M $Bu_4N[PF_6]$, scan rate 100 mV s^{-1}).

The oxidation of **4a** occurred as a diffusion-controlled, reversible redox transition at 0.08 V, whereas the oxidation of freshly prepared **6a** was detected at 0.05 V (Fig. 5). Conversely, the primary oxidation of complex **12** was anodically shifted to 0.25 V, although the characteristics of a one-electron reversible redox transition were maintained. These results were consistent with the cationic nature of the complex, which inherently renders electron removal more difficult. No oxidation corresponding to a possible Ru^{II}-to-Ru^{III} transition was observed within the accessible potential range.[34]

Considering their nature, the discussed redox processes were tentatively attributed to ferrocene/ferrocenium redox transitions and this assignment was corroborated by the DFT calculations of **1**, **3a**, and **12**. The calculations showed that the highest occupied molecular orbitals (HOMOs) of these molecules were predominantly localised on the ferrocene unit (see Fig. 6 and ESI†) and that the change in electron density associated with electron removal[35] exclusively occurred at the ferrocene unit.

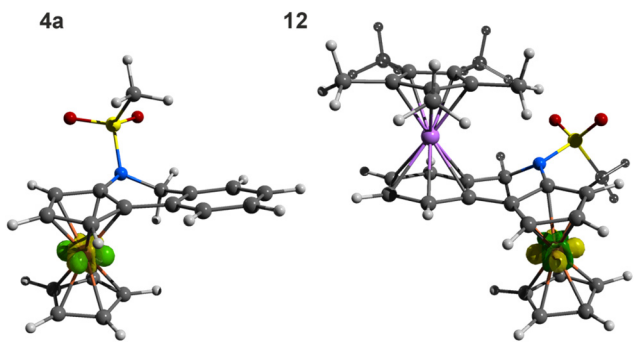

Fig. 6 Electron density changes associated with electron removal, $\rho(M^+) - \rho(M)$, mapped at the geometry of the parent species M (M = **4a** and the cation of **12**); isosurfaces at ±0.02 a.u. are shown. For details, see the ESI.†

Conclusion

In summary, we have developed a protocol for Pd-catalysed intramolecular C–H bond activation/C–C bond formation suitable for converting readily accessible *N*-[(bromoaryl)methyl]-*N*-(methylsulfonyl)aminoferrocenes into 1,2-dihydro-2-(methylsulfonyl)ferroceno[*c*]isoquinoline and the homologous compounds with one or two additional benzene rings *ortho*-fused onto the dihydroisoquinoline moiety. This method expands not only the palette of synthetic methods leading to planar-chiral ferrocenes annellated with N-heterocyclic moieties[9,36] but also the family of rare helical molecules containing a pivotal ferrocene moiety.[37] Attempts to perform the cyclisation reaction in an asymmetric manner using chiral phosphines as auxiliary ligands failed, but the compounds could be efficiently resolved into enantiomers using chromatography with chiral stationary phases. In addition, we demonstrated that the terminal ring in the model compound *N*-(methylsulfonyl)-1,2-dihydro-2-(methylsulfonyl)ferroceno[*c*]isoquinoline could be coordinated to the $(\eta^5\text{-}C_5Me_5)Ru^+$ fragment and that the ferrocenodihydroisoquinolines could be transformed into the corresponding isoquinolines. Unfortunately, the latter compounds readily degraded, which made further reactivity studies impossible.

Data availability

The data supporting this article have been included as part of the ESI.†

Conflicts of interest

The authors have no conflicts of interest.

Acknowledgements

This work was supported by the Charles University Research Centre Program (project no. UNCE/24/SCI/010). Computational resources were provided through the e-INFRA CZ project (ID: 90254), supported by the Ministry of Education, Youth and Sports of the Czech Republic.

References

1 Representative reviews:(*a*) R. Jazzar, J. Hitce, A. Renaudat, J. Sofack-Kreutzer and O. Baudoin, *Chem. – Eur. J.*, 2010, **16**, 2654; (*b*) T. W. Lyons and M. S. Sanford, *Chem. Rev.*, 2010, **110**, 1147; (*c*) L. Ackermann, *Chem. Rev.*, 2011, **111**, 1315; (*d*) T. Gensch, M. N. Hopkinson, F. Glorius and J. Wencel-Delord, *Chem. Soc. Rev.*, 2016, **45**, 2900; (*e*) F. Roudesly, J. Oble and G. Poli, *J. Mol. Catal. A: Chem.*, 2017, **426**, 275; (*f*) T. Rogge, N. Kaplaneris, N. Chatani, J. Kim, S. Chang, B. Punji, L. L. Schafer, D. G. Musaev,

J. Wencel-Delord, C. A. Roberts, R. Sarpong, Z. E. Wilson, M. A. Brimble, M. J. Johansson and L. Ackermann, *Nat. Rev. Methods Primers*, 2021, **1**, 43; (*g*) J. H. Docherty, T. M. Lister, G. Mcarthur, M. T. Findlay, P. Domingo-Legarda, J. Kenyon, S. Choudhary and I. Larrosa, *Chem. Rev.*, 2023, **123**, 7692.

2 (*a*) P. Štěpnička, *Dalton Trans.*, 2022, **51**, 8085; (*b*) *Ferrocenes: Ligands, Materials and Biomolecules*, ed. P. Štěpnička, Wiley, Chichester, 2008.

3 Selected reviews:(*a*) L. A. López and E. López, *Dalton Trans.*, 2015, **44**, 10128; (*b*) D.-Y. Zhu, P. Chen and J.-B. Xia, *ChemCatChem*, 2016, **8**, 68; (*c*) D.-W. Gao, Q. Gu, C. Zheng and S.-L. You, *Acc. Chem. Res.*, 2017, **50**, 351; (*d*) C.-X. Liu, Q. Gu and S.-L. You, *Trends Chem.*, 2020, **2**, 737; (*e*) Z.-Z. Zhang, D.-Y. Huang and B.-F. Shi, *Org. Biomol. Chem.*, 2022, **20**, 4061; (*f*) T. Čarný and R. Šebesta, *Synlett*, 2024, 165–182.

4 E. O. Fischer and D. Seus, *Z. Naturforsch.*, 1953, **8b**, 694.

5 D. E. Bublitz, W. E. McEwen and J. Kleinberg, *J. Am. Chem. Soc.*, 1962, **84**, 1845.

6 M. Cais, A. Modiano and A. Raveh, *J. Am. Chem. Soc.*, 1965, **87**, 5607.

7 (*a*) D.-W. Gao, Q. Yin, Q. Gu and S.-L. You, *J. Am. Chem. Soc.*, 2014, **136**, 4841; (*b*) R. Deng, Y. Huang, X. Ma, G. Li, R. Zhu, B. Wang, Y.-B. Kang and Z. Gu, *J. Am. Chem. Soc.*, 2014, **136**, 4472.

8 D.-W. Gao, C. Zheng, Q. Gu and S.-L. You, *Organometallics*, 2015, **34**, 4618.

9 For a review of ferrocene-fused nitrogen heterocycles, see: O. Bernardo, S. González-Pelayo and L. A. López, *Eur. J. Inorg. Chem.*, 2022, e202100911.

10 S. Luo, Z. Xiong, Y. Lu and Q. Zhu, *Org. Lett.*, 2018, **20**, 1837.

11 A.-A. Zhang, C. Chen, Y. Gao, M. Mo, R.-Z. Shen, Y.-H. Zhang, N. Ishida, M. Murakami and L. Liu, *Green Synth. Catal.*, 2021, **2**, 311.

12 (*a*) X. Ma and Z. Gu, *RSC Adv.*, 2014, **4**, 36241; (*b*) L. Liu, A.-A. Zhang, R.-J. Zhao, F. Li, T.-J. Meng, N. Ishida, M. Murakami and W.-X. Zhao, *Org. Lett.*, 2014, **16**, 5336; (*c*) L. Liu, H. Liu, Z. Zuo, A.-A. Zhang, Z. Li, T. Meng, W. Wu, Y. Hua and G. Mao, *Chin. Chem. Lett.*, 2021, **32**, 239.

13 W. Han, X. Zhou, S. Yang, G. Xiang, B. Cui and Y. Chen, *J. Org. Chem.*, 2015, **80**, 11580.

14 For the preparation of an analogous compound bearing a phosphine substituent at the ferrocene unit, see: V. Varmužová, F. Horký and P. Štěpnička, *New J. Chem.*, 2021, **45**, 3319.

15 Only minor amounts of **4a** were detected in the crude reaction mixtures obtained at 100 or 140 °C. Signals due to **6a** were detected in neither case..

16 (*a*) N. C. Bruno, M. T. Tudge and S. L. Buchwald, *Chem. Sci.*, 2013, **4**, 916; (*b*) N. C. Bruno, N. Niljianskul and S. L. Buchwald, *J. Org. Chem.*, 2014, **79**, 4161.

17 S. Ricard and A. Gagnon, *e-EROS Encyclopedia of Reagents for Organic Synthesis*, 2016, pp. 1–14; accessible through DOI: 10.1002/047084289X.rn01905.

18 I. Caivano, S. Bingel, I. Císařová, D. Nečas and M. Kotora, *Catal. Today*, 2022, **390–391**, 48.

19 (*a*) S. Wu, C. Liu, G. Luo, Z. Jin, P. Zheng and Y. R. Chi, *Angew. Chem., Int. Ed.*, 2019, **58**, 18410; (*b*) Y.-Y. Li, S. Li, T. Fan, Z.-J. Zhang, J. Song and L.-Z. Gong, *ACS Catal.*, 2021, **11**, 14388.

20 10 equiv. of Red-Al were used and the reaction was conducted in toluene at 0 °C/12 h and at room temperature/24 h. The reaction mixture contained only **6a** (30 and 35%, respectively) and the unreacted starting material.

21 M. Gingras, G. Félix and R. Peresutti, *Chem. Soc. Rev.*, 2013, **42**, 1007.

22 (*a*) L. T. Taylor, *J. Supercrit. Fluids*, 2009, **47**, 566; (*b*) K. De Klerck, De. Mangelings and Y. Vander Heyden, *J. Pharm. Biomed. Anal.*, 2012, **69**, 77; (*c*) C. West, *TrAC, Trends Anal. Chem.*, 2019, **120**, 115648; (*d*) D. Speybrouck, M. Howsam and E. Lipka, *TrAC, Trends Anal. Chem.*, 2020, **133**, 116090.

23 D. C. D. Butler and C. J. Richards, *Organometallics*, 2002, **21**, 5433.

24 (*a*) J. N. Baxter, J. Cymerman-Craig and J. B. Willis, *J. Chem. Soc.*, 1955, 669; (*b*) A. R. Katritzky and R. A. Jones, *J. Chem. Soc.*, 1960, 4497.

25 U. Salzner, *J. Chem. Theory Comput.*, 2013, **9**, 4064.

26 (*a*) D. R. Scott and R. S. Becker, *J. Chem. Phys.*, 1961, **35**, 516; (*b*) A. T. Armstrong, F. Smith, E. Elder and S. P. McGlynn, *J. Chem. Phys.*, 1967, **46**, 4321.

27 J. B. M. Somers, J. H. Borkent and W. H. Laarhoven, *Recl. Trav. Chim. Pays-Bas*, 1981, **100**, 110.

28 C. Slugovc, E. Rüba, R. Schmid, K. Kirchner and K. Mereiter, *Monatsh. Chem.*, 2000, **131**, 1241.

29 K. Nakamoto, *Infrared and Raman Spectra of Inorganic and Coordination Compounds, Part A: Theory and Applications in Inorganic Chemistry, 6th edition*, Wiley, Hoboken, 2009, ch. 2.8, pp. 221–237.

30 G. Albertin, S. Antoniutti, J. Castro and G. Gasparetto, *New J. Chem.*, 2019, **43**, 2676.

31 (*a*) M. J. S. Dewar, *Bull. Soc. Chem. Fr.*, 1951, **18**, C71; (*b*) J. Chatt and L. A. Duncanson, *J. Chem. Soc.*, 1953, 2939.

32 (*a*) G. Gritzner and J. Kůta, *Pure Appl. Chem.*, 1984, **56**, 461; (*b*) R. R. Gagné, C. A. Koval and G. C. Lisensky, *Inorg. Chem.*, 1980, **19**, 2854.

33 C. Hansch, A. Leo and R. W. Taft, *Chem. Rev.*, 1991, **91**, 165.

34 Electrochemical oxidation of $[(\eta^5\text{-}C_5Me_5)Ru(\eta^6\text{-}C_6H_6)]^+$ in MeCN/0.1 M $Bu_4N[BF_4]$ was detected at +2.11 V *vs*. SCE: O. V. Gusev, M. A. Ievlev, M. G. Peterleitner, S. M. Peregudova, L. I. Denisovich, P. V. Petrovskii and N. A. Ustynyuk, *J. Organomet. Chem.*, 1997, **534**, 57.

35 (*a*) J. Schulz, F. Uhlík, J. M. Speck, I. Císařová, H. Lang and P. Štěpnička, *Organometallics*, 2014, **33**, 5020; (*b*) K. Škoch, I. Císařová, F. Uhlík and P. Štěpnička, *Dalton Trans.*, 2018, **47**, 16082; (*c*) K. Škoch, J. Schulz, I. Císařová and P. Štěpnička, *Organometallics*, 2019, **38**, 3060; (*d*) P. Vosáhlo, J. Schulz, I. Císařová and P. Štěpnička, *Dalton Trans.*, 2021, **50**, 6232; (*e*) M. Franc, J. Schulz and P. Štěpnička, *Dalton Trans.*, 2024, **53**, 11445.

36 Relevant recent examples:(*a*) V. Mamane and Y. Fort, *J. Org. Chem.*, 2005, **70**, 8220; (*b*) J. Wang, Z.-H. Zhu, M.-W. Chen, Q.-A. Chen and Y.-G. Zhou, *Angew. Chem., Int. Ed.*, 2019, **58**, 1813; (*c*) Z.-B. Zhao, X. Li, M.-W. Chen, Z. K. Zhao and Y.-G. Zhou, *Chem. Commun.*, 2020, **56**, 7309; (*d*) M. Ito, M. Okamura, K. S. Kanyiva and T. Shibata, *Organometallics*, 2019, **38**, 4029; (*e*) K. Yoshida, Q. Liu, R. Yasue, S. Wada, R. Kimura, T. Konishi and M. Ogasawara, *ACS Catal.*, 2020, **10**, 292; (*f*) Y. An, X.-Y. Zhang, Y.-N. Ding, Y. Li, X.-Y. Liu and Y.-M. Liang, *Org. Lett.*, 2022, **24**, 7294; (*g*) N. Lin, B. Hong, J. Zhao and Z. Gu, *Angew. Chem., Int. Ed.*, 2023, **62**, e202215530.

37 Selected examples:(*a*) N. Saleh, C. Shen and J. Crassous, *Chem. Sci.*, 2014, **5**, 3680 (review); (*b*) A. Urbano, G. Hernández-Torres, A. M. del Hoyo, A. Martínez-Carrión and M. C. Carreño, *Chem. Commun.*, 2016, **52**, 6419; (*c*) T. Shibata, N. Uno, T. Sasaki and K. S. Kanyiva, *J. Org. Chem.*, 2016, **81**, 6266; (*d*) M. Akiyama and K. Nozaki, *Angew. Chem., Int. Ed.*, 2017, **56**, 2040; (*e*) A. Urbano, A. M. del Hoyo, A. Martínez-Carrión and M. C. Carreño, *Org. Lett.*, 2019, **21**, 4623.